Dill, R., Dobslaw, H., Thomas, M. (2019): Improved 90-day Earth orientation predictions from angular momentum forecasts of atmosphere, ocean, and terrestrial hydrosphere. - *Journal of Geodesy*, *93*, 3, pp. 287—295.

DOI: http://doi.org/10.1007/s00190-018-1158-7

Journal of Geodesy manuscript No.
(will be inserted by the editor)

Improved 90-day Earth orientation predictions from angular momentum forecasts of atmosphere, ocean, and terrestrial hydrosphere

R. Dill · H. Dobslaw · M. Thomas

Received: date / Accepted: date

Abstract Short-term forecasts of atmospheric, oceanic, and hydrological effective angular momentum functions (EAM) of Earth rotation excitation are combined with least-squares extrapolation and auto-regressive modeling to routinely predict polar motion (PM) and ΔUT1 for up to 90 days into the future. Based on hindcast experiments covering the years 2016 and 2017, a best-performing parametrization was elaborated. At forecast horizons of 10 days, remaining prediction errors are 3.02 mas and 5.39 mas for PM and ΔUT1, respectively, corresponding to improvements of 34.5 % and 44.7 % when compared to predictions reported routinely in Bulletin A of the International Earth Rotation and Reference Systems Service. At forecast horizons of 60 days, prediction errors are 12.52 mas and 107.96 mas for PM and ΔUT1, corresponding to improvements of 34.5 % and 8.2 % over Bulletin A. The 90 days-long EAM forecasts leading to those improved EOP predictions are routinely published on a daily basis at isdc.gfz-potsdam.de/esmdata/eam.

Keywords Earth Rotation Prediction · Polar Motion and Length-of-Day Variations · Effective Angular Momentum Functions · AAM, OAM, HAM

1 Introduction

Changes of the Earth's orientation with respect to inertial space as defined by the position of the rotation axis (polar motion; PM) and changes in the angular velocity (ΔUT1) are caused by external gravitational forces and geodynamical processes that exchange angular momentum between the solid Earth and its fluid envelope. Atmospheric winds and surface pressure changes as represented by current numerical weather models explain almost 90 % of the observed changes in ΔUT1 (e.g. *Gross et al.*, 2004). PM is excited equally by atmospheric and oceanic dynamics and to a smaller extent by changes in the terrestrial water storage (TWS). In particular, large-scale variations in water masses on the continents are responsible for seasonal excitations in PM and ΔUT1.

Effective angular momentum (EAM) functions summarize the excitation of Earth orientation changes due to atmosphere, ocean, and the terrestrial hydrosphere. The equatorial EAM components χ_1, χ_2 excite PM, the axial component χ_3 quantifies ΔUT1. The International Earth Rotation and Reference Systems Service (IERS; https://www.iers.org/IERS/EN/DataProducts/GeophysicalFluidsData/geoFluids.html) provides a comprehensive list of publicly available model-based EAM for the atmosphere (AAM), ocean (OAM), and terrestrial water (HAM). Many studies analysed, compared, or even combined such EAM data sets in great detail (e.g. *Brzezinski*, 1992; *Gross et al.*, 2004; *Chen and Wilson*, 2005; *Zhou et al.*, 2005; *Brzezinski et al.*, 2009; *Chen et al.*, 2012; *Nastula et al.*, 2012).

Predicted Earth orientation parameters (EOP) are important for various operational purposes including navigation of deep-space satellite missions, the pointing of astronomical instruments, or satellite-based positioning on Earth. Assuming that regular updates of EOP predictions are made available frequently, most applications require forecasts for only some days into the future. For occasional users of Global Navigation Satellite Systems (GNSS), however, it is important to have such predictions available for a longer period, so that

R . Dill
Section 1.3: Earth System Modelling, Helmholtz Centre Potsdam - GFZ German Research Centre for Geosciences
E-mail: dill@gfz-potsdam.de

the availability of valid predictions and consequently quicker re-acquisition of satellite signals are ensured even after a longer offline period of a certain device. During the past, many innovative prediction methods have been applied to EOP, including artificial neural networks or fuzzy inference systems (e.g. *Petrov et al.*, 1995; *Schuh et al.*, 2002; *Akyilmaz and Kutterer*, 2004). More recent efforts (e.g. *Xu et al.*, 2012; *Shen et al.*, 2017; *Wang*, 2017) emphasize the ongoing necessity for improved EOP predictions, particularly for forecast horizons below 30 days.

The short-term EOP prediction error can be significantly reduced by considering not only AAM data as routinely included into ΔUT1 predictions (*Johnson et al.*, 2005; *Dick and Richter*, 2009), but also OAM and HAM data for both PM and ΔUT1 (*Dill and Dobslaw*, 2010). To incorporate those short-term AAM, OAM, and HAM forecasts into EOP predictions, the model-based EAMs have to be transformed into PM and ΔUT1 time series. As model-based EAMs suffer from biases and un-modeled processes, the resulting EOPs show reasonable prediction skills only for short-term high-frequency variations (*Dobslaw and Dill*, 2018), but not for seasonal or Chandler wobble variations and the trend. *Dill and Dobslaw* (2013) achieved improvements for the 90-day forecast horizon using a skill-weighted patching of 10-day EOP forecasts calculated from modeled EAMs and the 90-day EOP predictions reported routinely in Bulletin A prepared by the IERS Rapid Service/Prediction Centre at the U.S. Naval Observatory (*Stamatakos et al.*, 2011). This prediction combination reflects the high-frequency variations from the model-based short-term forecasts and the seasonal and long-term signals from Bulletin A slightly upgraded in their offset and trend according to the improved short-term forecast.

In this paper, we follow a more rigorous way to exploit the modeled 6-day EAM forecasts for 90-day EOP predictions. We stay in the domain of Earth rotation excitation functions and extrapolate a single EAM time series that represents a projection of the total Earth rotation excitation (GAM; geodetic angular momentum function) without the need of any other prediction products like Bulletin A. From this EAM prediction, the EOP prediction can be obtained via the Liouville equation by starting the integration of the EAM time series into EOPs from the most recently observed EOPs. The essential step in the following prediction scheme is the introduction of the geodetic residual, the difference between observed geodetic and modeled geophysical excitation, to assess seasonal variations (offset, trend, annual and it's higher harmonics) that are not covered by the hydrodynamic models. The potential contributions of geophysical excitations and geodetic residuals are discussed in terms of significant frequencies in Sect. 2. The model-based 6-day EAM forecasts together with the geodetic residual, derived from past years of observed EOPs, are than projected for 90 days into the future by least-squares extrapolation (LS) and auto-regressive modeling (AR). For a set of 550 hindcasts covering the years 2016 and 2017, the effects of different parametrization choices for LS and AR are evaluated in terms of their impact on the prediction accuracy (Sect. 3). The best-performing prediction is subsequently evaluated by calculating EOP forecasts from the 90-day EAM predictions and comparing them to Bulletin A one-by-one for each of the hindcasts (Sect. 4). Sect. 5 summarizes the results and gives some concluding remarks.

2 Comparison of Geodetic and Geophysical Excitations

We utilize a set of geophysical EAM functions as provided by the Earth System Modelling group of GFZ Potsdam (ESMGFZ) via isdc.gfz-potsdam.de/esmdata/eam (*Dobslaw et al.*, 2010). In addition to the usually considered AAM, OAM, and HAM, we are also including so-called barystatic Sea-Level Angular Momentum functions (SLAM) that account for global mass balance effects and the associated sea-level changes. As discussed by *Chen* (2005) and *Yan and Chao* (2012), most combinations of AAM+OAM+HAM do not account for global mass conservation. Atmospheric and hydrological mass variations are generally not compensated by freshwater fluxes within a combined atmosphere-land-ocean model system. General circulation ocean models typically conserve volume or mass. However, consideration of global mass conservation is not only essential for the annual excitation budget in ΔUT1, but has also a non-negligible effect on annual PM excitation. For the period 1976 - 2016, we estimate amplitude spectra for all periods up to 400 days. For comparison we use the latest realisation of the EOP 14 C04 series (*Bizouard and Gambis*, 2008) as delivered by the IERS to derive GAM by means of the Liouville equation (e.g. *Barnes et al.*, 1983; *Brzezinski*, 1992). Effects of long-period tides are removed from the GAM ΔUT1 component as recommended in the IERS conventions (*Petit and Luzum*, 2010, Table 8.1).

For most of the frequencies in all three EAM components $\chi_{1,2,3}$, the magnitudes of the residuals are substantially lower than the observations from C04, implying that a considerable amount of the signal is explained

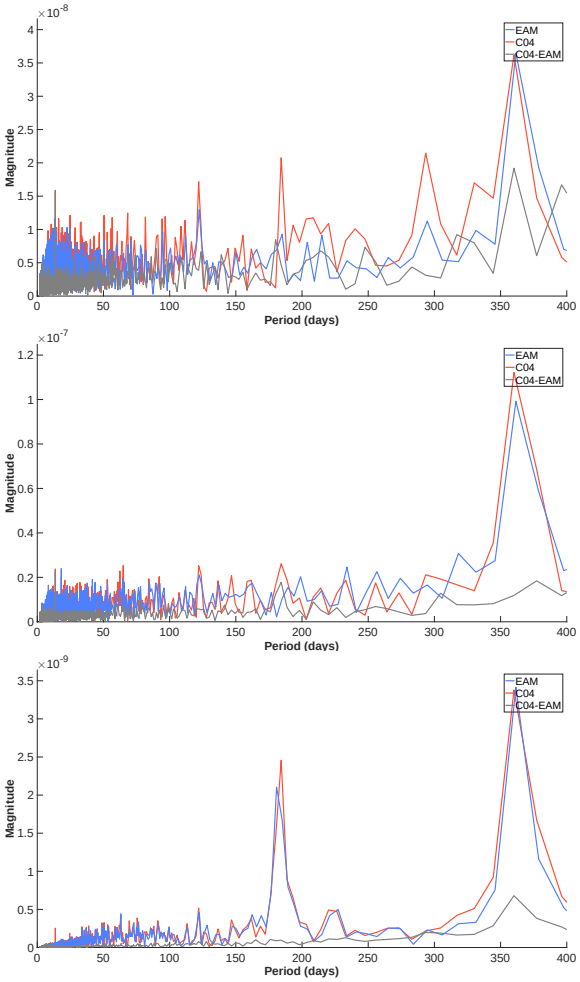

Fig. 1 Fourier spectrum of geodetic excitation GAM from C04 (red), modeled angular momentum function EAM=AAM+OAM+HAM+SLAM (blue) and the residual GAM-EAM (gray): χ_1 (top), χ_2 (middle), χ_3 (bottom).

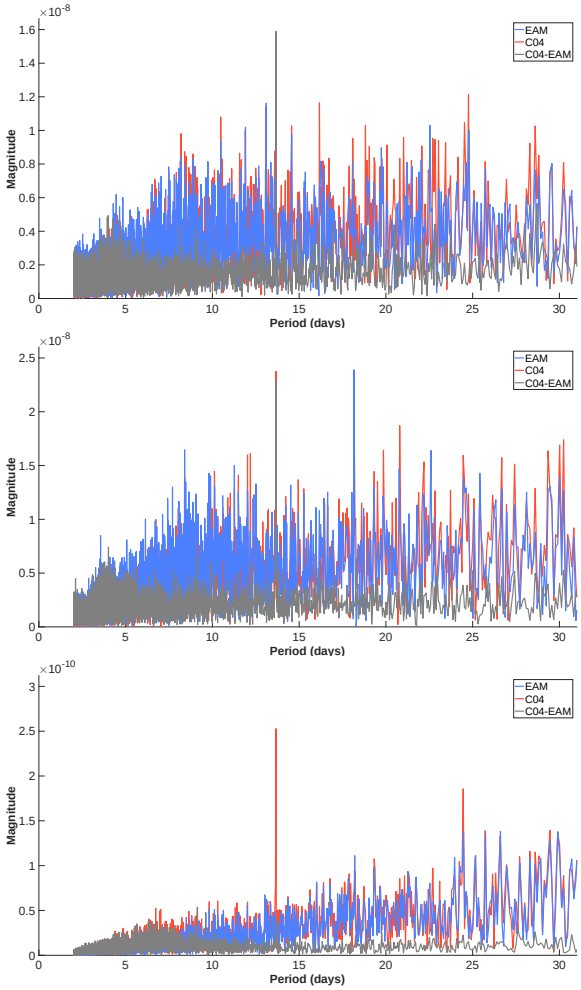

Fig. 2 Sub-monthly Fourier spectrum of geodetic excitation GAM from C04 (red), modeled angular momentum function EAM=AAM+OAM+HAM+SLAM (blue) and the residual GAM-EAM (gray): χ_1 (top), χ_2 (middle), χ_3 (bottom).

by the geophysical model (Fig. 1). Notable residuals are left at the annual frequency and its associated higher harmonics in particular for the PM components. For periods shorter than 100 days, we note various distinct peaks in GAM that are not present in the geophysical excitations. Those peaks are most prominent in χ_1, but can also be identified in the other two components.

When looking specifically into the high-frequency range of the spectra (Fig. 2), we note a distinct peak at 13.7 d in all three GAM components that is not explained by the geophysical EAM. More peaks are visible in individual components only, as e.g. 2.9 d in χ_1, 3.8 d in χ_2, and 9.3 d in χ_3 that are not reproduced by the geophysical models.

ΔUT1 and PM are strongly affected by tidal effects. Since diurnal and semi-diurnal tidal contributions excited in the models due to atmospheric pressure forcing were removed during data processing of ESMGFZ, the model-based EAM functions represent only the non-tidal geophysical excitation. Usually, tidal signals at diurnal and semi-diurnal frequencies are also removed during geodetic data processing by applying the sub-daily tide model recommended by IERS (*Petit and Luzum*, 2010). In addition, we applied the IERS tidal model for ΔUT1 to reduce the long-periodic tides from GAM χ_3, too. In PM however, all tidal signals with periods above 1 day remain in the time series due to the lack of readily available correction models. Furthermore, all applied tidal models are not free from errors *Madzak et al.* (2016). Sub-daily tidal variations and further systematic effects with periodic behavior have been also identified in recent EOP estimates obtained by the International GNSS Service (IGS; *Ray et al.*, 2017). Similarly, *Ray and Erofeeva* (2014) found residual tidal energy not reduced by the IERS ΔUT1 tidal model for the lunar tide at 18.6 y and 9.3 y, for the solar con-

stituents at 365.25 d and 182.6 d, as well as for the fortnightly Mf constituent with 13.7 d and the Mt with 9.1 d. Hence, GAM, and in consequence the residuals between GAM and EAM, are not completely free of tidal contributions. Since in this study we want to predict Earth rotation comparable to C04 and Bulletin A, we consequently include the most prominent periodicities seen in the residuals, into our set of frequencies for the least squares extrapolation, see following section.

3 Prediction of Effective Angular Momentum

The abilities of different ERP prediction approaches have been thoroughly assessed with the international Earth Orientation Prediction Comparison Campaign (EOPPCC; *Kalarus et al.*, 2010). For the seasonal prediction horizon, a combination of least squares estimation and autoregressive modeling (LS+AR) turned out to be the most reliable method. For short-term prediction horizons, the incorporation of AAM forecasts into the prediction, particularly by means of a Kalman Filter (*Chin et al.*, 2009) yield substantially more accurate predictions than any other method.

We rely on those findings of the EOPPCC and attempt to utilize LS+AR in combination with geophysical forecasts. In contrast to previous work, however, we do not predict PM and ΔUT1 directly but focus on EAM predictions instead, which can be subsequently integrated in time via the Liouville equation from arbitrary initial values to obtain EOPs for future epochs. EAMs are essentially time derivatives of EOPs, thus, the predicted EOPs are much more sensitive to the extrapolation of the non-harmonic signals in the EAMs than extrapolating offset and trend in the EOPs. As discussed before, model-based EAM functions are not able to represent the total GAM. In contrast to the approach presented by *Dill and Dobslaw* (2013), where Bulletin A supplies the missing seasonal signal, we use the geodetic residual to complement the model-based EAMs, and are therefore independent of an EOP prediction product from another source. Because EOP observations that are necessary to derive GAM are available only with some latency, we extrapolate the geodetic residual from the last available date of EOP observations to the end of the 6-day EAM forecasts.

The 90-day EAM prediction is then composed of two steps: (A) extrapolation of the residuals between GAM and EAM until 6 days into the future, when only the deterministic geophysical forecasts are available; and (B) for all days after day 6, when the full EAM signals (modeled EAM + GAM residual) have to be forecasted. For both extrapolation steps we use LS+AR. For LS we set up the seasonal periods 1 y, 1/2 y, 1/3 y. Furthermore, as the residuals between GAM and EAM contain also tidal and draconitic signals, we included the 13.7 d period and additionally only for the axial component also 9.13 d, 27.4 d, 3.0 y, and 9.3 y. The two equatorial excitation components are predicted together as 2D vector $\chi_1 + i\chi_2$ as they are interrelated by the Liouville equation.

For part (A), the sum of all individually modeled final EAM functions from atmosphere, oceans and the terrestrial hydrosphere from the past four years are combined with the latest 6-day forecasts and averaged to arrive at daily values sampled at 12 h UTC. GAM is obtained from C04 augmented by the IERS rapid solutions, each as long as it is available. For the most recent 4 years of data overlap of both series, the residual between GAM and EAM is calculated. All frequencies indicated above are estimated from this time interval and are subsequently extrapolated forward in time. AR is then applied to the remaining residuals that are obtained after subtracting the LS fit. For part (B), LS+AR is applied to the full EAM signal obtained from the 3-hourly modeled EAM and the extrapolated GAM residual resampled to 3 h.

For both, LS and AR, a number adjustable parameters exist that might influence the quality of the resulting predictions. Those particularly include (i) the time-span of the harmonic analysis; (ii) the time-span for the estimation of offset and trend; (iii) the time-span for the auto-regression model; and (iv) the length (i.e., order) of the autoregression model. We perform up a huge number of hindcast experiments to test the influence of different parameter sets on LS and AR. For each experiment, covering the years 2016 and 2017 with 550 individual prediction runs, we integrated the EAM predictions to EOP predictions starting at the EOP coordinates given in Bulletin A at day 0. Finally, we selected a set of parameters that leads to smallest RMS errors for forecasts in the range of 1 - 30 days when contrasted against C04 (Tab. 1). Comparable parameters for LS and AR were also used by *Kosek et al.* (2005) and *Niedzielski and Kosek* (2008) for EOP predictions.

To demonstrate the relative importance of the different parameters on the forecast quality, we present results from 10 additional experiments (P1 - P10) in which we alter those parameters over a wide range of possible choices (Fig. 3 and Fig. 4). We note that both PM and ΔUT1 are in particular degraded when the trend of the full EAM signal in Part (B) is estimated over a longer period of 2 or even 4 years, see experiments P6+P7 in Fig. 3 and P5+P6 in Fig. 4. All other processing choices are of rather minor importance for the prediction accuracies.

	Part (A) residuals GAM - model EAM	Part (B) full EAM
	$\chi_1 + i\chi_2$	
time span for harmonic analysis	4 years	4 years
time span for offset and trend	1 year	1 year
time span for AR model	2 years	1 year
order of AR model	20 days	2 days
	χ_3	
time span for harmonic analysis	4 years	4 years
time span for offset and trend	4 years	1 years
time span for AR model	4 years	2 years
order of AR model	60 days	25 days

Table 1 Parameters selected for least squares (LS) extrapolation and the autoregressive (AR) modeling applied in the 90 days-long EAM forecasts as provided by ESMGFZ. The number of coefficients for the AR order is multiplied by the sampling rate to give the effective AR length in days.

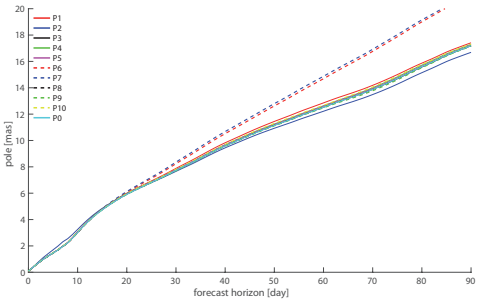

Fig. 3 RMS for pole offset for different parameter choices for LS and AR. P0: Reference experiment as specified in Tab. 1. P1: trend for residuals from the last 100 days. P2: trend for residuals from last 4 years. P3: AR order 5 for residuals. P4: AR order 60 for residuals. P5: AR for residuals from last 1 year. P6: trend for full EAM from 2 years. P7: trend for full EAM from 3 years. P8: AR order 8 for full EAM. P9: AR order 200 for full EAM. P10: no AR for residuals and full EAM.

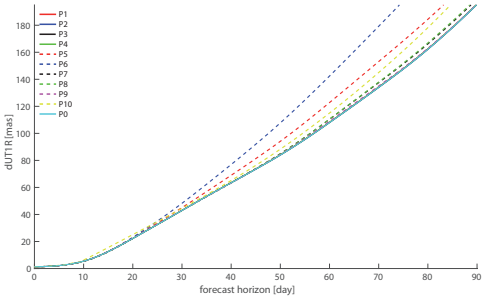

Fig. 4 RMS for ΔUT1 for different parameter choices for LS and AR. P0: Reference experiment as specified in Tab. 1. P1: trend for residuals from the last 1 year. P2: trend for residuals from last 2 years. P3: AR order 20 for residuals. P4: AR order 80 for residuals. P5: trend for full EAM from 4 years. P6: trend for full EAM from 2 years. P7: AR order 20 for full EAM. P8: AR order 60 for full EAM. P9: AR order 100 for full EAM. P10: no AR for residuals and full EAM. All EOP components are consistently expressed in angular units mas, 15 mas correspond to 1 ms of ΔUT1.

4 Comparison with Bulletin A

Prediction results with LS and AR as parametrized according to Tab. 1 are finally compared with Bulletin A for each forecast individually (Fig. 5). Prediction errors, expressed as differences between prediction and the final reference solution C04, reveal episodic features that can be predicted neither by ESMGFZ nor Bulletin A. Note that both, PM and ΔUT1 are expressed in angular units of milliarcseconds, where 15 mas correspond to 1 ms of ΔUT1. Differences in the x-component are slightly higher than in the y-component. The spread in Bulletin A with -45 mas to +23 mas in x-pole and -33 to +30 mas in y-pole is greater than for ESMGFZ with -37 to +24 mas (x-pole) and -23 to +21 mas (y-pole). The signs of ESMGFZ prediction differences do not always conform with the signs of the Bulletin A prediction differences. Within consecutive predictions, it is apparent that episodic features migrate from prediction day 90 down towards day 1. For very short-term predictions (i.e., below 10 days), ESMGFZ is able to predict such signals due to the inclusion of 6-day dynamic model forecasts. The prediction differences in ΔUT1 are also reduced in ESMGFZ spreading from -492 to +74 mas compared to Bulletin A with -526 to +299 mas. Both predictions contain epochs with clusters of increased prediction errors but those epochs do not always coincide among ESMGFZ and Bulletin A.

Fig. 6 gives the amount of improved or degraded ESMGFZ predictions when compared to Bulletin A. For each 90-day prediction, the forecast errors are summarized by root mean squares for short-term predictions (day 1-10), monthly predictions (day 10-40), and seasonal predictions (day 40-90). Negative signs indicate that ESMGFZ errors are lower than Bulletin A errors. For polar motion the reduction of the absolute value of the complex noted error difference is given. For all components ESMGFZ provides significantly more improved forecasts than degraded ones, especially in the

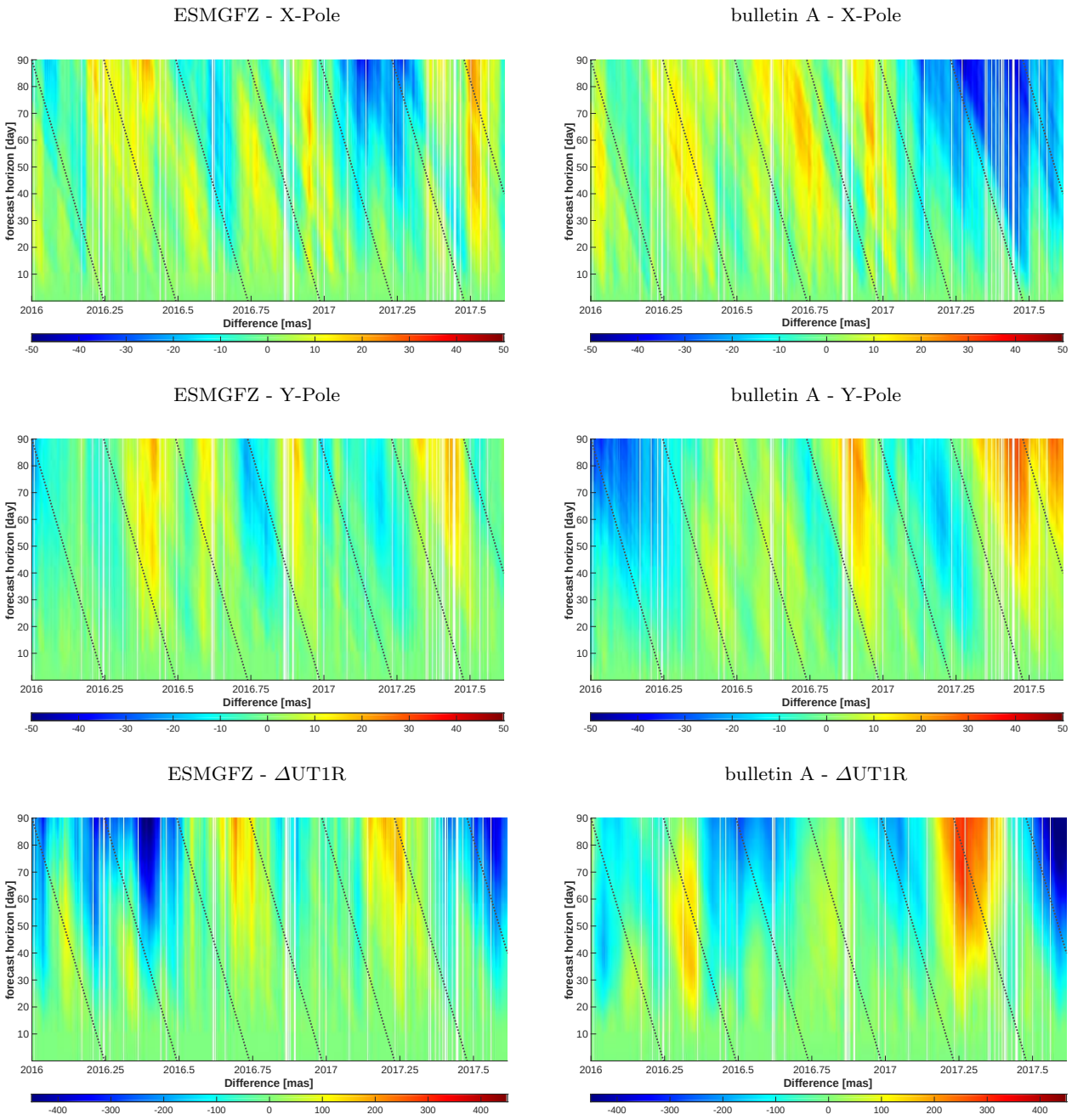

Fig. 5 Difference in [mas] for predictions of ESMGFZ (left) and Bulletin A (right) up to 90 days into the future compared to C04 computed at 550 different starting epochs. Polar motion x-component (top), y-component (middle), and ΔUT1R (bottom). All EOP components are consistently expressed in angular units mas, 15 mas correspond to 1 ms of ΔUT1R.

short-term range. Moreover, ESMGFZ predictions with reduced errors outweigh the predictions with increased errors not only in quantity but also in quality. This conclusion holds also for the monthly and seasonal prediction horizon.

Tab. 2 summarizes the forecast accuracies of ESMGFZ and Bulletin A. Since initial conditions were always taken from Bulletin A to allow for a fair comparison, numbers for day 0 are equal for both approaches. From day 1 to day 10, ESMGFZ benefits from the 6-day hydrodynamic model forecasts with significantly reduced RMS errors. The improvement in y-pole (44.9 %) is slightly higher than for the x-pole (41.3 %). ΔUT1 is also improved by 44.7 % indicating that OAM and to a lesser extent also HAM do not only contribute to PM excitation but also noticeably to length-of-day variations. From day 6 onward, ESMGFZ predictions yield still reduced RMS values when compared to Bulletin

	0 days	1 day	5 days	10 days	20 days	40 days	60 days	90 days
x-pole								
ESMGFZ [mas]	0.08	0.33	1.25	2.56	5.01	7.58	9.43	14.31
Bulletin A [mas]	0.08	0.35	2.13	3.89	6.21	10.26	13.26	17.21
reduction [%]	0.0	5.7	41.3	34.2	19.3	26.1	28.7	16.9
y-pole								
ESMGFZ [mas]	0.04	0.23	0.75	1.59	3.15	5.87	8.25	9.51
Bulletin A [mas]	0.04	0.24	1.36	2.48	4.47	8.15	11.52	15.86
reduction [%]	0.0	4.2	44.9	35.9	29.5	28.0	28.4	40.0
pole								
ESMGFZ [mas]	0.09	0.40	1.46	3.02	5.91	9.59	12.52	17.19
Bulletin A [mas]	0.09	0.43	2.53	4.61	7.64	13.11	17.57	23.40
reduction [%]	0.0	7.0	42.3	34.5	22.6	26.9	28.7	26.5
UT1								
ESMGFZ [mas]	1.35	1.36	2.09	5.39	22.17	63.34	107.96	195.16
Bulletin A [mas]	1.35	1.80	3.31	9.75	29.84	74.73	120.17	188.55
reduction [%]	0.0	24.4	36.9	44.7	25.6	13.9	8.2	-3.5

Table 2 RMS prediction error [mas] compared to C04 for polar motion and ΔUT1R from 550 hindcast experiments at forecast horizons of 0, 1, 5, 10, 20, 40, 60, and 90 days for ESMGFZ (1st row) and Bulletin A (2nd row). Last row gives the error reduction [%] of ESMGFZ over Bulletin A. All EOP components are consistently expressed in angular units mas, 15 mas correspond to 1 ms in UT1.

A, although both time series use comparable prediction methods (LS+AR). In PM the RMS values are reduced by about 26.9 % at day 40 and still 26.5 % at day 90. The main two differences between Bulletin A predictions and our predictions are the additional information about the geophysical fluids excitation for 6 days into future and the extrapolation in the EAM domain instead of the EOP domain. Supposing that long-term harmonic signals are captured by ESMGFZ and Bulletin A more or less similarly we conclude that ESMGFZ is able to detect short-term and high-frequency deviations from the long-term periodic signal within the most recent geophysical excitation that have a lasting positive influence on the EOP prediction integrated for 90 days into the future. Obvious improvements in single EOP prediction time series are a smaller offset at forecast day 6 and a better fit in the short-term (<90 days) trend. In that context, the PM predictions benefit certainly most from the updated state of the oceanic excitation.

5 Summary

Hydrodynamic models of the atmosphere, ocean, and terrestrial water storage provide valuable information for short-term Earth rotation prediction. Moreover, 6-day forecasts of geophysical Earth orientation excitation from such models have useful prediction skills to extend routinely processed Earth rotation excitation time series beyond present day. At sub-daily to seasonal time scales Earth rotation predictions based on modeled Earth rotation excitation series are able to reduce the EOP prediction error significantly.

Introducing the geodetic residual excitation as difference between Earth rotation excitation derived from latest observations and the sum of all hydrodynamic modeled excitation contributions, periodic signals not fully captured by the geophysical fluid models can be recovered from the past years and extrapolated into the epochs where only the 6-day model forecasts but no EOP observations are available. Model-based excitations and extrapolated geodetic residuals, representing together Earth's full effective angular momentum function, is subsequently extrapolated from the end of the 6-day forecasts up to 90 days into the future. Along with the daily update of the model-based 6-day EAM forecasts, ESMGFZ provides this seasonal 90-day EAM prediction routinely on its FTP server.

Applying the Liouville equation, Earth rotation predictions can be calculated from this EAM predictions in a straightforward way. Besides accurate EAM predictions, it is necessary to start the integration of EAM into EOP from the best available geodetic estimate of the orientation of the Earth. Ultra-Rapid geodetic EOP solutions with reduced accuracy as calculated for example by the International GPS Service (IGS) provide nowadays initial EOP coordinates with a few hours latency only. In recent years the deviation of the broadcasted initial day coordinates from the final EOP coordinates was reduced from about 1 mas to less than 0.3 mas (*Gross and Ratcliff*, 2016) due to optimizations in the IGS processing chain. Further important improvements in short-term Earth rotation prediction could be expected from reduced forecasts errors in the atmospheric mass and wind fields. Seasonal PM and especially ΔUT1 prediction are also very sensitive to the accuracy of global mass exchanges between atmosphere,

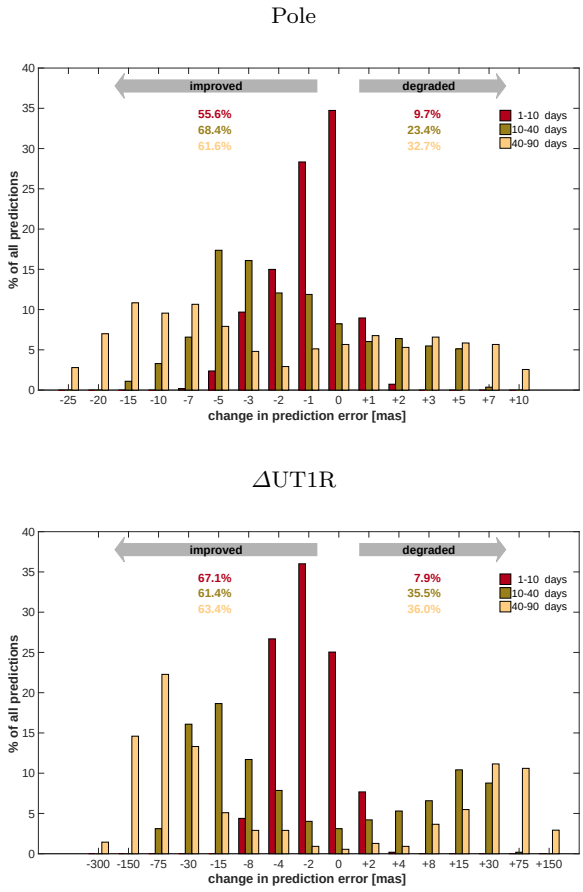

Fig. 6 Histogram of differences in prediction errors between Bulletin A and ESMGFZ. Prediction error differences (negativ means smaller error) are calculated for 550 individual 90-day predictions as RMS of the differences for short-term predictions (1-10 days), monthly predictions (10-40 days), and seasonal prediction (40-90 days). All EOP components are consistently expressed in angular units mas, 15 mas correspond to 1 ms of ΔUT1R. Numbers give sums of improved and degraded predictions.

ocean, and land. The SLAM forecast data could be further improved by considering global seasonal ocean mass distributions, derived from the Gravity Recovery and Climate Experiment (GRACE) satellite mission (*Wahr et al.*, 1998; *Cheng et al.*, 2011; *Nastula et al.*, 2015), to geographically locate the excess masses from atmosphere and terrestrial water storage. Apart from the approach used in this study, alternative strategies to incorporate EAM functions into Earth rotation predictions, as e.g. Kalman filter or multivariate autoregressive techniques (*Kosek*, 2012) might offer possibilities to further improve the EOP prediction accuracy while incorporating forecasted EAM.

References

Akyilmaz O, Kutterer H (2004) Prediction of Earth rotation parameters by fuzzy inference systems, J. of Geodesy, Volume 78, Issue 12, pp 8293, 10.1007/s00190-004-0374-5.

Barnes RTH, Hide A, White A, Wilson CA (1983) Atmospheric angular-momentum fluctuations, Length-Of-Day changes and Polar Motion. Proc. R. Soc. London Ser. A-Math. Phys. Eng. Sci., 387, 1792, pp 31-73.

Bizouard C, Gambis D (2008) The combined solution C04 for Earth orientation parameters, recent improvements. In: Drewes, H. (ed), Series on International Association of Geodesy Symposia, 134, pp 330, Springer, New York.

Brzezinski A, Nastuala J, Kolaczek B (2009) Seasonal excitation of polar motion estimated from recent geophysical models and observations. J. of Geodynamics, 48, 235-240, 10.1016/j.jog.2009.09.021

Brzezinski A (1992) Polar motion excitation by variations of the effective angular momentum function: considerations concerning deconvolution problem. Manuscripta geodaetica, 17, pp 3-20.

Chen JL, Wilson CR (2005) Hydrological excitations of polar motion, 1993-2002. Geophys. J. Int., 160, pp 833-839.

Chen JL (2005) Global mass balance and the length-of-day variation. J. Geophys. Res., 110, B08404, 10.1029/2004JB003474.

Chen JL, Wilson CR, Zhou YH (2012) Seasonal excitation of polar motion. J. Geodyn., 62 , pp 8-15, 10.1016/j.jog.2011.12.002.

Cheng M, Ries JC, Tapley BD (2011) Variations of the Earth's figure axis from satellite laser ranging and GRACE. J. Geophys. Res., 116, B01409, 10.1029/2010JB000850.

Chin TM, Gross RS, Boggs DH, Ratcliff JT(2009) Dynamical and Observation Models in the Kalman Earth Orientation Filter. IPN Progress Report, pp 42-176.

Dick WR, Richter B (2009) Earth Orientation Centre. IERS Annual Report 2007, pp 61-67, International Earth Rotation and Reference Systems Service, Central Bureau. Frankfurt am Main: Verlag des Bundesamts für Kartographie und Geodäsie, ISBN 978-3-89888-917-9.

Dill R, Dobslaw H (2010) Short-term Polar Motion Forecasts from Earth System Modeling Data. J. of Geodesy, 84, 9, pp 529-536, 10.1007/s00190-010-0391-5.

Dill R, Dobslaw H, Thomas M (2013) Combination of modeled short-term angular momentum function

forecasts from atmosphere, ocean, and hydrology with 90-day EOP predictions. J. of Geodesy. 2013, pp 567-577.

Dobslaw H, Dill R, Grötzsch A, Brzezinski A, Thomas M (2010) Seasonal polar motion excitation from numerical models of atmosphere, ocean, and continental hydrosphere. J. Geophys. Res., 115, B10, 406, 10.1029/2009JB007127.

Dobslaw H, Dill R (2018) Predicting Earth Rotation Variations from Global Forecasts of Atmosphere-Hydrosphere Dynamics. Advances in Space Research, 10.1016/j.asr.2017.11.044.

Gross RS, Fukumori I, Menemenlis D, Gegout P (2004) Atmospheric and oceanic excitation of length-of-day variations during 1980-2000. J. Geophys. Res., 109, B01406.

Gross RS, Ratcliff JT (2016) Improving Near Real-Time and Predicted Earth Orientation Parameters Using IGS Ultra-Rapid Polar Motion and Length-of-Day Measurements. IGS Workshop 2016: GNSS Futures, Sydney, Australia; February 8-12, 2016.

Johnson TJ, Luzum BJ, Ray JR (2005) Improved near-term UT1R predictions using forecasts of atmospheric angular momentum. J. of Geodynamics, 39, pp 209-221.

Kalarus M, Schuh H, Kosek W, Akyilmaz O, Bizouard C, Gambis D, Gross R, Jovanovi B, Kumakshev S, Kutterer H, Mendes Cerveira PJ, Pasynok S, Zotov L (2010) Achievements of the Earth orientation parameters prediction comparison campaign. J. of Geodesy, 840, pp 587-596.

Kosek W, Kalarus M, Johnson TJ, Wooden WH, McCarthy DD, Popinski W (2005) A comparison of LOD and UT1-UTC forecasts by different combined prediction techniques. Artif. Satell., 40, pp 119-125.

Kosek W (2012) Future improvements in EOP prediction. Proc. IAG 2009 Scientific Assembly Geodesy for Planet Earth. S. Kenyon et al. (eds.), IAG Symposia Series Vol. 136, Springer-Verlag Heidelberg, pp 513-520.

Madzak M, Schindelegger M, Böhm J, Bosch W, Hagedoorn J (2016) High-frequency Earth rotation variations deduced from altimetry-based ocean tides. J. of Geodesy, 2016, 90, pp 1237-1253.

Niedzielski T, Kosek W (2008) Prediction of UT1-UTC, LOD and AAM χ_3 by combination of least-squares and multivariate stochastic methods. J. of Geodesy, 2008, 82, pp 83-92.

Nastula J, Gross R, Salstein DA (2012) Oceanic excitation of polar motion: Identification of specific oceanic areas important for polar motion excitation. J. of Geodynamics, 62, pp 16-23.

Nastula J, Salstein DA, Popiski W (2015) Hydrological excitations of polar motion from GRACE gravity field solutions. International Association of Geodesy Symposia, Springer Berlin Heidelberg.

Petit G, Luzum B (2010) IERS Conventions 2010, Tech. Note 36, International Earth rotation and reference systems service, Verlag des Bundesamts fr Kartographie und Geodäsie.

Petrov S, Brzezinski A, Gubanov V (1995) A Stochastic Model For Polar Motion With Application To Smoothing, Prediction, And Combining, ftp://haydn.cbk.waw.pl/pub/serge/petrov96.ps.gz

Ratcliff JT, Gross RS (2017) Combinations of Earth Orientation Measurements: SPACE2012, COMB2012, and POLE2012. JPL Publication, 13-16, https://ntrs.nasa.gov/search.jsp?R=20140011392 2017-12-14T14:31:04+00:00Z.

Ray RD, Erofeeva SY (2014) Long-period tidal variations in the length of day. J. Geophys. Res., 119, pp 1498-1509, 10.1002/2013JB010830.

Ray J, Rebischung P, Griffiths J (2017) IGS polar motion measurement accuracy. Geodesy and Geodynamics, Volume 8, Issue 6, pp 413-420, 10.1016/j.geog.2017.01.008

Shen Y, Guo J, Liu X, Wei X, Li W (2017) One hybrid model combining singular spectrum analysis and LS + ARMA for polar motion prediction. Advances in Space Research, 59(2), 513-523, 10.1016/j.asr.2016.10.023.

Schuh H, Ulrich M, Egger D, Müller J, Schwegmann W (2002) Prediction of Earth orientation parameters by artificial neural networks. J. of Geodesy, 76(5), 247-258. 10.1007/s00190-001-0242-5.

Stamatakos N, Luzum B, Stetzler B, Shumate N (2011). Recent improvements in the rapid service prediction center products for 2010 and 2011, 125128.

Wahr J, Molenaar M, Bryan F (1998) Time variability of the Earth's gravity field: hydrological and oceanic effects and their possible detection using GRACE. J. Geophys. Res., 103, B12, 30.

Wang G. (2017) Application of the radial basis function neural network to the short term prediction of the Earth s polar motion, Studia Geophysica et Geodaetica, November 2017, 10.1007/s11200-017-0805-4.

Xu XQ, Zotov L, Zhou YH (2012) Combined Prediction of Earth Orientation Parameters. China Satellite Navigation Conference (CSNC) 2012 Proceedings Lecture Notes in Electrical Engineering, 2012, Volume 160, Part 2, 361-369, 10.1007/978-3-642-29175-3-32.

Yan H, Chao BF (2011) Effect of global mass conservation among geophysical fluids on the seasonal length of day variation. J. of Geophys. Res., 117, B2, pp

2156-2202, 10.1029/2011JB008788.

Zhou YH, Chen JL, Liao XH, Wilson CR (2005) Oceanic excitations on polar motion: a cross comparison among models. Geophysical Journal International, 162, pp 390.